MedCrave
Step into the World of Research

International Robotics & Automation Journal

Research Article

Open Access

CrossMark

Design of active ankle foot orthotics for gait assistance and fall prevention

Abstract

An active ankle-foot orthosis (AAFO) was developed with the intent of providing propulsive ground reaction force to individuals at risk of experiencing fall. The device makes use of one double-acting cylinder per leg, and a lever arm system to transfer propulsive force to the ground, and potentially assist in fall prevention and rehabilitation. Preliminary tests have been shown to improve ground reaction forces in walking. In this paper, the design and construction of the device is included as well as the control algorithm used and testing procedure. This research may be used to advance the field of gait assistance and fall prevention through use of active foot orthotics.

Keywords: force, orthotics, gait, balance, field, propulsive, ground, reaction, deficits, trauma

Volume 6 Issue 3 - 2020

Jason Olson,[1] Sambarta Ray,[2] Thomas Sugar,[1] Claire Honeycutt,[3] Sangram Redkar[1]

[1]Department of engineering, Arizona state university, USA
[2]Department of electrical engineering, Arizona state university, USA
[3]Department of biomedical engineering, Arizona state university, USA

Correspondence: Sangram Redkar, Department of engineering, Fulton Schools of Engineering, Arizona State University, Tempe, AZ 85281, USA, Tel 480-727-1129, Fax 480-727-1125, Email sredar@asu.edu

Received: August 08, 2020 | **Published:** August 27, 2020

Introduction

Falls occur when a person is unable to maintain postural control and collides with their surroundings. Falls most commonly result in soft tissue damage and in more severe cases fractures and death. Along with physical injuries, falls can also cause psychological trauma, associated with fear of falling that can lead to deficits in gait and balance, reduced physical activities and deconditioning.[1]

Certain groups of people are more susceptible to experience fall than others, one of which being stroke survivors. Although the risk of stroke increases with age, a stroke can occur at any age, and the most common type of stroke inhibits blood flow to the brain.[2] The brain is responsible for sending motor signals to muscles through the nervous system required for muscle movement. After a stroke, these signals get affected and can delay muscle, both kinetic and kinematic responses to perturbation.[1] Partial or complete loss of muscle activity (paresis) in the lower limb or limbs can result in some cases. This loss of muscle activity leads to motor-issues such as Drop foot (i.e. inability to lift the impaired foot during swing phase of gait) or Spasticity (i.e. stiffness and tightening of muscles) of lower limb muscles. These issues lead to the loss of postural control[3] increasing fall risk among those affected. Stroke is not uncommon either, with around 795,000 people in the United States suffering from stroke annually according to the Centers for Disease Control and Prevention (CDC). Falls are the common complaints that individuals with such impairment have during or after their rehabilitation phase. Statistics on after stroke falls[4] reveal that 14%-65% patients fall during hospitalization and between 37%-73% fall during the first 6 months of discharge from hospital. The most commonly prescribed clinical remedy provided to tackle drop foot issue and improper gait is passive thermoplastic Ankle Foot Orthosis (AFO) that is designed to lock the paretic ankle joint at a certain angle, facilitate foot clearance during swing phase, ankle stability during stance phase and heel strike. While there are reported improvements of gait velocity, stride length and cadence(steps/min) shown after the use of such AFOs, studies[5] show that continual constraints in the ankle joint adversely affects the compensatory stepping response, forward propulsion and proprioceptive sensory information. The primary contributor to the kinetic energy and the speed of the stepping leg is forward propulsion force which is generated by the plantar flexor muscles. Locking the ankle joint using rigid AFOs lead to impeded forward propulsion due to restricted plantar flexion and that can cause inhibited compensatory stepping response, inadequate foot clearance and improper gait. Therefore, there is a need for an Active Ankle Foot Orthotics (AAFO) which can deliver powered push off for a stronger plantar flexion, locking of the ankle joint during swing phase to prevent dragging of the paretic foot and a stable heel strike.

Orthotics researchers have sought to build such a device to help those with lower body impairments. This has been accomplished either by simply furthering the knowledge level in the field, or by producing a device capable of assisting in either muscle augmentation or rehabilitation. One such study by Yamamoto et al. detailed a semi-active AFO device aimed at hemiplegic patients who used specialized joints using stiffness control elements, flexion stops, and a one-way friction clutch to control ankle movement in the sagittal plane.[6] The AFO was tested on 33 subjects, and information was discovered with regard to what AFO characteristics were most needed with hemiplegic patients.[6] A pneumatic power-harvesting ankle-foot orthosis is described by Chin et al.,2009,[7] which attempts to combat foot-drop issues in subjects with lower-body motor-control disruptions.[7] The design incorporates a bellow pump below the foot, and a cam-lock mechanism is used to control relative ankle motion.[7] Results of the testing performed on an able-bodied subject indicated that the locking mechanism used needs further refinement as excess dorsiflexion of the ankle was observed.[7] An active AFO studied in Palmer used a linear torsional spring for controlling plantar flexion.[8] The spring would acquire elastic energy during the loading of the stance phase and would release this energy during the pre-swing (push-off) phase to generate forward propulsion in the user. The device was tested on 10 healthy subjects and demonstrated that passive spring force actuation is insufficient in providing comparable power to that of a biological ankle.[8] The AAFO by Hwang et al, 2006,[9] shows use of a

Series Elastic Actuator (SEA) to control ankle actuation for toe drag and foot drop prevention. The SEA makes use of an elastic element in series with a motor to generate a controlled movement of the ankle. The device was tested on five healthy subjects, and was able to successfully prevent the toe drag of test subjects during the swing phase.[9] Similarly, Boehler et al, 2008,[10] describes an AAFO designed for rehabilitation applications which also uses a SEA as a means of actuation. The device also allows for the user to wear their existing shoes, although due to its fastening method limiting ankle motion to the sagittal plane, the device is limiting with regard to user comfort and maneuverability.[10] Testing was performed on a single subject, and results indicated promising open-loop control results for the novel algorithm used. Polinkovsky et al, 2012,[11] describes another AFO which makes use of SEA actuation to restore legged motion in patients suffering from a spinal cord injury. The AAFO was able to reduce toe drag and foot slap of the spinal cord injury subject test users, but was mechanically unable to apply maximum torque or maximum throw in able-bodied subjects in anything faster than a slow walk.[11] Ferris et al, 2005,[12] presented a powered AFO which made use of McKibben style pneumatic muscles for actuation, and was built as a gait studying tool for post neurological injury rehabilitation. The device was shown to produce both plantarflexion and dorsiflexion of the ankle joint.[12] It was designed such that it can be externally supplied with electrical power and compressed air, and testing results indicated that its use in physical therapy clinics may reduce the level of manual labor required by physical therapists.[12] The effectiveness in active ankle flexion motivated the design of the device in this paper.

In this paper, we propose an unobtrusive, cost effective, easy to wear, active AFO which is designed using double acting pneumatic cylinders for actuation, Inertial Measurement Units (IMUs) for sensing the leg motion and a custom 3D printed shoe attachment. The proposed AFO attaches the barrel of the cylinder to the shank of the user using padded braces, and the moving piston to the ankle attachment which is fixed to the shoe of the user using screws. The system detects the user's leg in motion by using the Euler angles in the sagittal plane (i.e., longitudinal anatomical place which divides a human body into left and right parts) obtained from IMU sensors which are also attached to the front of the user's shank.

System design and modelling

Design of the mechanical system

The AAFO's design takes a mechanical approach to supplement the Soleus and gastrocnemius muscles in a controlled manner, while allowing for maximum range of motion and comfort of the user. The design offers reasonable accommodation to a variety of users with respect to shoe size and weight and can be quickly adjusted such that it does not reduce range of motion of the ankle. Adjustments are made either through replacement of the lever arm, as well as tightening or loosening of the turnbuckle connecting rods. These adjustments allow the AAFO to operate at up to approximately 25 degrees of Dorsiflexion, and up to approximately 70 degrees of plantarflexion. The connecting rods use swivel-ball ends which allow some degree of foot rotation as well as inversion and eversion of the foot. The dorsiflexion and plantar flexion angles can be seen in Figure 1. The AAFO uses 8 self-tapping screws to secure it to a running or walking shoe and can be adapted to fit a range of shoe sizes and styles. This ability increases user comfort, affordability, and accessibility.

The AAFO uses a lever arm that is allowed to pivot in the middle around a steel pin and is fixed at one end to the fore end of the user's shoe with two screws. The pivot point of the arm is secured to the hind end of the user's shoe with the remaining 6 screws, and the other end of the lever arm is attached to a double acting air cylinder where retraction and extension forces are applied. Simple geometric relationships can be used to derive the relationship between input air pressure and maximum theoretical propulsive force.

$$F_{GR} = cos(\theta) \times P_{air} \times A_{cylinder} \times \frac{d_1}{d_2}$$

$$F_{GR} = \cos(\theta) x\, P_{air}\ \text{x5.34}$$

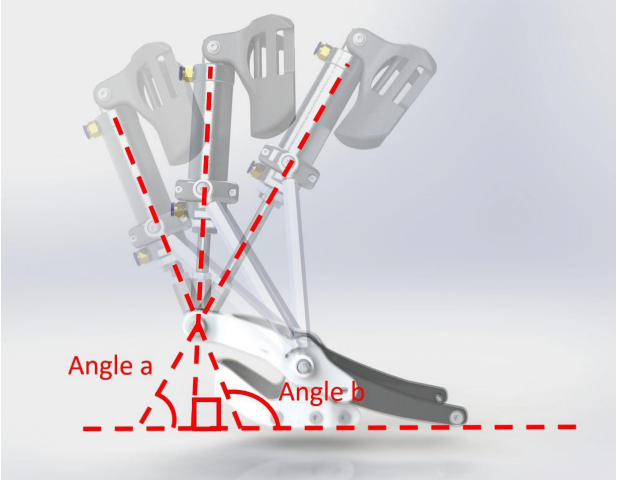

Figure 1 Maximum variation of angle for Plantar- and Dorsi-flexion.

The application of the force on the mechanical parts of the design can be seen from Figure 2. The equation above can be used to calculate the maximum theoretical propulsive force the AAFO. With a cylinder bore of approximately 32 mm, and a maximum pressure of approximately 70 psi, the maximum theoretical force the AAFO can provide is approximately 287.28 N. Using 4.25 mm inner diameter hoses, approximately 1.37 m in length from the air solenoid, the response time of the actuator system is approximately 0.104 seconds. This is a limiting factor for the system in terms of user agility, as it is not suitable for typical human running speed. Human agility in terms of terrain angle however should not be limited by the device, as it offers a high degree of abduction, adduction, inversion, and aversion. To minimize the weight being added to the lower extremities, much of the pneumatics of the system were moved remotely to reduce the negative metabolic effects of increased weight to the lower legs. A Condor Modular Operator Plate Carrier (MOPC) was used to house the pneumatic control equipment for the suit including the air solenoids, batteries, and all electronics except for the sensors and the AAFOs themselves. The Air solenoids used were Numatics 236127B 24V 6Watt Solenoid valves and were responsible for control of the air flow through the system. The sensor casings and much of the AAFO parts except for the air cylinder and hardware were 3D printed in polylactic acid material. The double-acting air cylinder used was a Sydien Single Rod Double Action Pneumatic Cylinder with a 32mm Bore and a stroke of 75 mm.

Air was supplied via a commercial air compressor located remotely. A mobile air supply system would be similarly effective at delivering propulsive force as well and was successfully tested. The mobile air supply system can be seen in Figure 3. The design and orientation of the lever arm, linkage arms, and shank support provides a rigid connection between the shank and foot with minimal chafing or rubbing.

Citation: Olson J, Ray S, Sugar T, et al. Design of active ankle foot orthotics for gait assistance and fall prevention. *Int Rob Auto J.* 2020;6(3):106–113. DOI: 10.15406/iratj.2020.06.00209

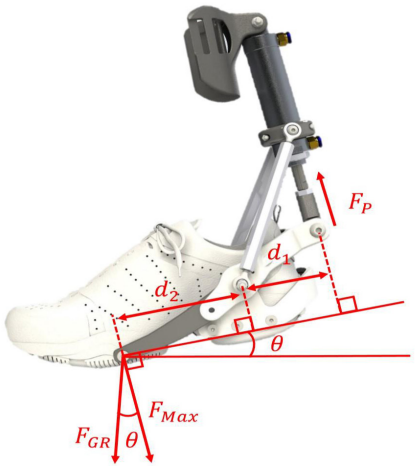

Figure 2 Geometric representation of the force acting on the shoe.

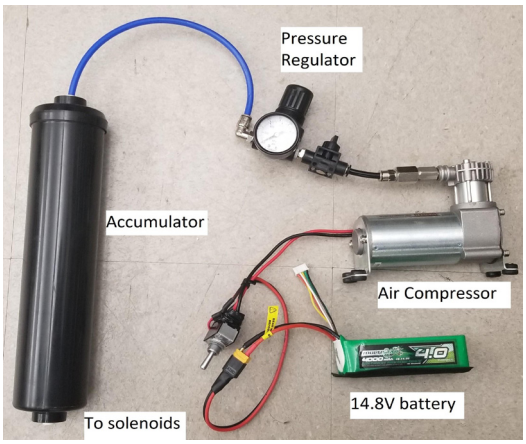

Figure 3 Mobile air supply with accumulator and pressure regulator.

The force of the air cylinder contracting is transferred through the level arm to the front of the foot, where the foot typically reaches maximum Plantar flexion at the beginning of the swing phase, ensuring maximum propulsive force duration.

Design of the electronic system

The AAFO uses an Adafruit Feather HUZZAH with ESP8266 processor on board to process and transmit the incoming IMU data for data analysis on computers via WiFi, as well as output control signals to two VNH5019 motor driver carriers. The motor drivers are responsible for activating the air solenoid valves and thus control the pneumatic actuation of the AAFO. The IMUs used are two Adafruit (Adafruit Industries, New York, NY) BNO055 absolute orientation sensors which are placed on the shank of the subjects using straps and custom designed sensor housing. The paper from Quintero et al, 2017,[13] showed a similar application of using IMU sensors for detecting gait cycles for lower orthotics. The feather Huzzah is programmed using the Arduino IDE and a MATLAB (Mathworks, Natick, MA) script is developed to remotely acquire the data via WiFi. The IMU sensor is a 9-DOF sensor with 3-axis accelerometer, gyroscope and magnetometer.

System block diagram

In Figure 4 we show the block diagram of the system. The V_1, V_2, V_3 and V_4 are the solenoid valves that control the actuation of two cylinders. The IMU's communicate with the Microcontroller on the I2C (Inter-Integrated Circuit) communication bus with clock and data lines. There is an internal 10k pull up resistor on the IMU board. The pull-up resistors provide the default states of the signal lines.

Control algorithm

We designed an algorithm 1 for controlling the actuation of the cylinder based on the Euler angle inputs from the IMU sensors. The V_1, V_2, V_3 and V_4 are the solenoid valves shown in Figure 4. We used the connection diagram mentioned in Qi H, et al, 2019,[14] for finalizing the solenoid connections. The control parameters defined in the algorithm are described as follows.

α is the threshold angle for the absolute difference of the angles between the two IMUs. α_1 is the left shank angle and α_2 is the right shank angle with respect to the vertical plane from the sagittal side. λ is the flag that determines which leg needs to be actuated. It's set to 1 left leg and 2 for the right leg. This ensures that a single leg is not actuated consecutively during a single gait cycle.

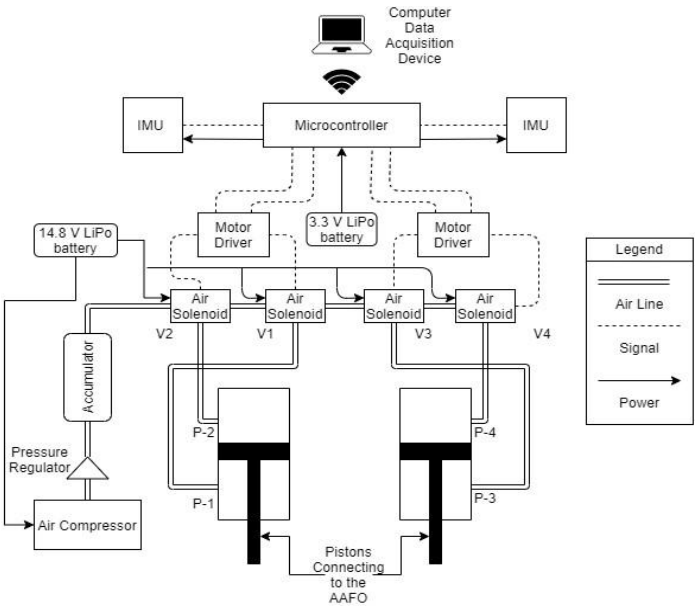

Figure 4 Block Diagram of the system.

Citation: Olson J, Ray S, Sugar T, et al. Design of active ankle foot orthotics for gait assistance and fall prevention. *Int Rob Auto J.* 2020;6(3):106–113. DOI: 10.15406/iratj.2020.06.00209

τ is the time delay for the sensor read. This was set to the minimum amount possible for consistent data communication over Wifi for the data acquisition system. t_0, t_1 and t_2, these are time set for determining the various phases of the gait cycle. Since, we conducted our experiment at a constant speed, the values remained constant throughout the experiment.

Algorithm 1 Control algorithm for the device

Initialize: Sensor system, Wifi module, calibration parameters, control parameters like α, λ,τ,t_0, t_1 and t_2. Obtain offset values from calibration parameters for the sensors

while Client connected **do**

Obtain α_1 and α_2 from IMU sensors {Retrieve the Euler angles from IMU sensors}

if $abs(\alpha_1 - \alpha_2) > \alpha$ **then**

if $\alpha_1 < \alpha_2$ and $\lambda \sim= 1$ **then**

Activate V_1 {Extend Left leg for push off}

Start counter $t = t_1$

Set $\lambda = 1$ {Here *lambda* = 1 indicates left leg}

else if $\alpha_1 > \alpha_2$ and $\lambda \sim= 2$ **then**

Activate V_3 {Extend Right leg for push off}

Start counter $t = t_1$

Set $\lambda = 2$ {Here *lambda* = 2 indicates right leg}

end if

else

Deactivate V_1, V_2, V_3 and V_4 {Free move state}

end if

Reduce counter t

if $t < t_2$ **then**

if $\lambda = 1$ **then**

Activate V_2 {Retract Left leg for heel strike}

end if

if $\lambda = 2$ then

Activate V_4 {Retract Right leg for heel strike}

end if

end if

wait for τ ms {Delay for sensor read}

end while

In Figure 5, we show the various phases of a single gait cycle as captured from the testing of the device by the subjects. The nomenclature of each of the phases was obtained from Taborri J, et al, 2016.[15] Here the phases are labeled according to the left leg of the subject (i.e. the leg closer to the camera). The angle α is the angle difference between the two IMU sensors placed in front of the shank of the subject. The sensors provide the shank angle on the sagittal plane of the subject. Here α is the control parameter used in our control algorithm 1. We obtain the shank angle measurements as shown in Figure 6. In the paper Watanabe t, et al, 2011,[16] the angle variation of the knee for each phase of the gait cycle is shown and using those values we were able to estimate the timings for actuation of the cylinders. We also confirmed the estimated values with the data obtained from our IMU sensors as shown in Figure 6 by observation during the habituation phase of the subjects to determine the values for the control parameters α, t_0, t_1 and t_2. These values were also adjusted according to the comfort of the subjects.

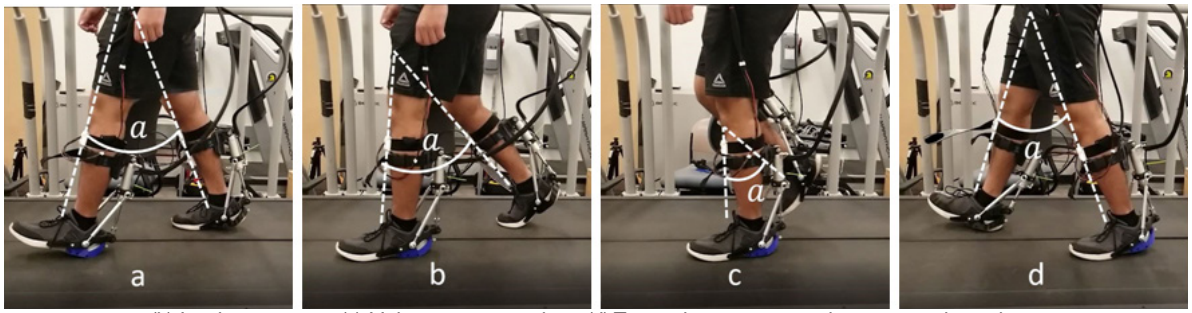

(a) Double support, stance (b) Loading response, (c) Mid stance, stance phase (d) Terminal stance, stance phase stance phase phase.

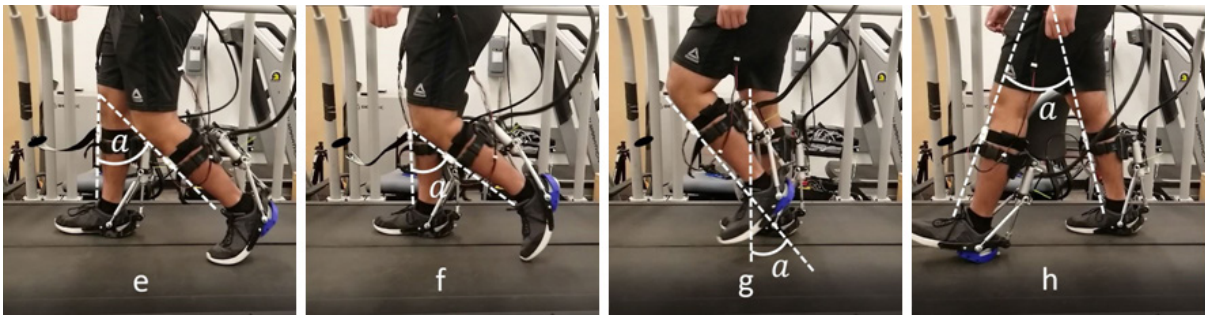

(e) Pre swing (Push-off), (f) Initial Swing, swing (g) Mid Swing, Swing (h) Terminal Swing (Heel stance phase phase phase strike), swing phase.

Figure 5 A single gait cycle with 8 level of granularity.

Citation: Olson J, Ray S, Sugar T, et al. Design of active ankle foot orthotics for gait assistance and fall prevention. *Int Rob Auto J.* 2020;6(3):106–113. DOI: 10.15406/iratj.2020.06.00209

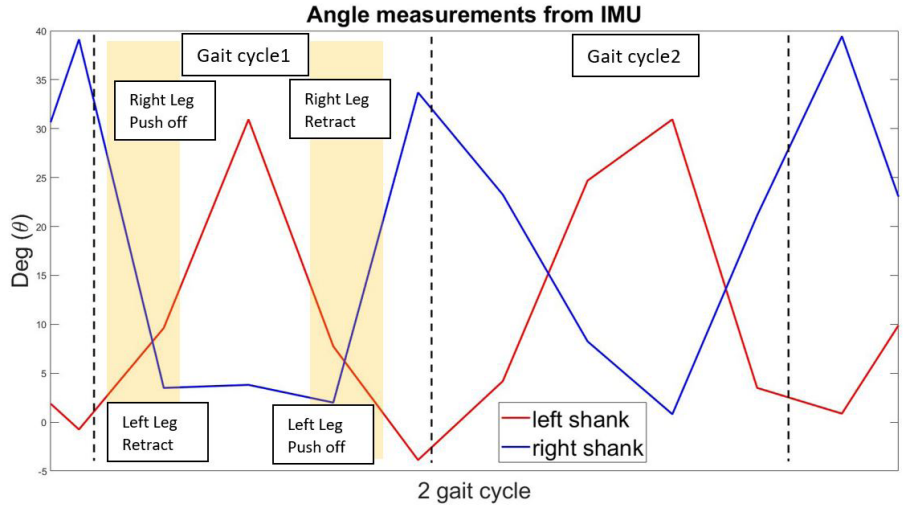

Figure 6 Shank angle measurement from IMU sensors.

Results and discussion

Testing procedure

After IRB approval, we conducted a preliminary test of our device's ability to provide a stronger plantar flexion, we used 4 subjects on an instrumental dual-belt treadmill with force sensors (Bertec, Columbus, Ohio). The subject was fitted with the device on both of their legs and were made to wear the condor plate carrier with all the additional equipment. The testing phase had two sessions.

i. Habituation Test for acclimatization to the device: In their first session the subjects were fitted with the AAFO and were made to walk on the ground for 5 minutes to habituate themselves with the device. They were given 10 minutes on the treadmill with varying speed between 0.5 m/s to 1.2 m/s to acclimate themselves to the shoes for the final testing session. During their habituation time on the treadmill, data of their shank angle variation was collected from the IMU sensors for estimating their plantar flexion time and their swing phase time for synchronizing the actuation of the cylinders. The source pressure varied from 30 psi to 70 psi and the subjects were notified about the pressure before to allow them to anticipate the assistance from the device.

ii. Walking test for collecting ground reaction force: In their second session, the subjects were instructed to walk on the treadmill for 1 min with both legs split on the right and left belt of the treadmill with normal walking speed of 1 m/s. A passive reflective heel marker was placed on both the heels of the subject to determine the heel strike event on the treadmill. The motion of the heel marker was captured using a motion capture system (Vicon, Oxford, UK) at 1000 Hz. There were 4 pressure conditions used for testing the ground reaction force:

a. No pressure,

b. Pressure at 30 psi,

c. Pressure at 50 psi,

d. Pressure at 70 psi.

Ground Reaction Force (GRF) was collected for each of the pressure used. We used young subjects of similar age group without any impairments for the purpose of this preliminary test. Subject information can be found in Table I.

Table 1 Subject attributes

Attributes	Sub A	Sub B	Sub C	Sub D
Height(cm)	177.8	172.2	177.8	185.4
Weight(kg)	88.45	87.54	87.99	112.35
Age	20	25	25	25
Shoe size (US)	11.5	9.0	9.5	12.0

Results of ground reaction force (GRF)

The Figures 7,8,9 & 10 represent the Anterior-Posterior GRF obtained from the left leg of the 4 subjects. The initial data from the motion capture system was processed in the Vicon Nexus software (Vicon, Oxford, UK), where the markers were labelled, and gaps were filled with a custom plugin.

The data was then extracted and further processed on the Matlab software (MathWorks, Natick, MA). The raw data was initially filtered with a 2nd order low pass butterworth filter of 10 Hz. The heel strike events were calculated by finding the recurrence of the least angle of the heel marker. The individual gait cycles were then extracted from the filtered data, they were then curve fitted to match the dimensions and an average of 5 gait cycles were taken to obtain the average plots. The plots show the GRF obtained for the 4 pressure conditions. The red line indicates the GRF at 0psi, green line indicates GRF at 30psi, blue line indicates GRF at 50psi and black line indicates GRF at 70psi. The GRF data of the Subject D at 70psi was a bad trial and was excluded from the plots. The initial trough in the plots is the Braking force applied by the stepping leg to go from the swing phase of the gait cycle to the stance phase after heel strike. The peak that follows from the trough represents the Propulsive force that the stepping foot generates to transfer from stance phase to swing phase of the gait cycle.

Citation: Olson J, Ray S, Sugar T, et al. Design of active ankle foot orthotics for gait assistance and fall prevention. *Int Rob Auto J.* 2020;6(3):106–113. DOI: 10.15406/iratj.2020.06.00209

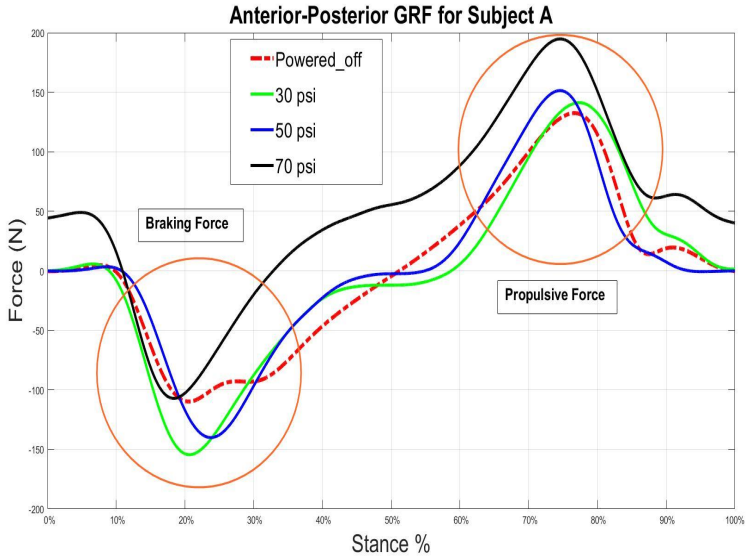

Figure 7 Anterior-Posterior GRF of left leg of Subject A.

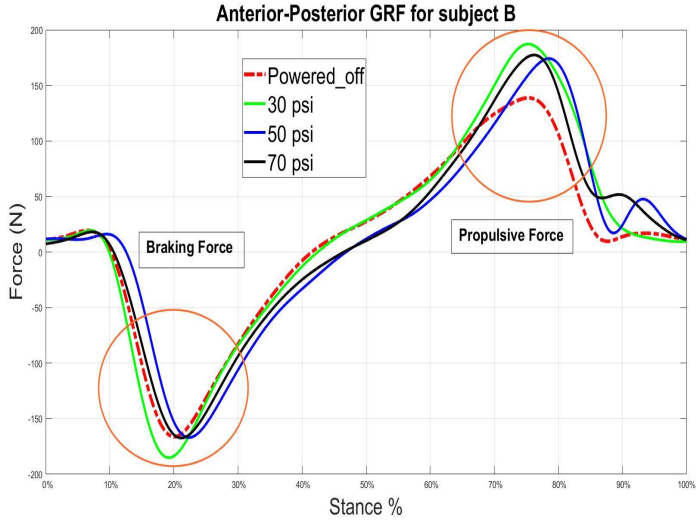

Figure 8 Anterior-Posterior GRF of left leg of Subject B.

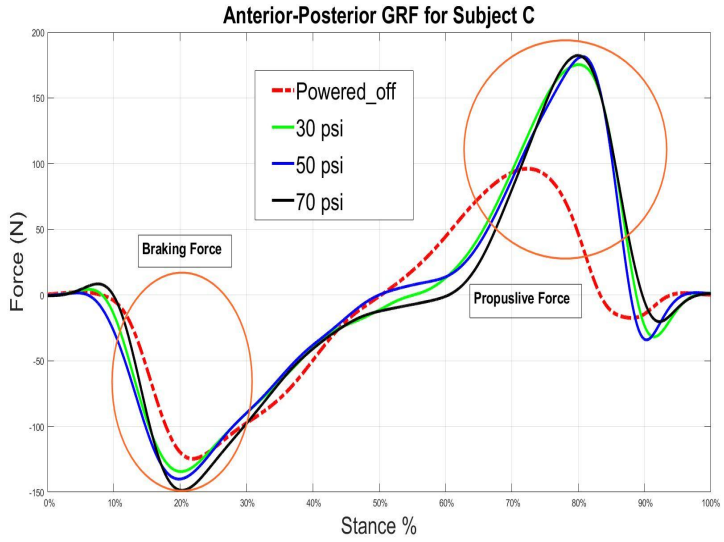

Figure 9 Anterior-Posterior GRF of left leg of Subject C.

Citation: Olson J, Ray S, Sugar T, et al. Design of active ankle foot orthotics for gait assistance and fall prevention. *Int Rob Auto J.* 2020;6(3):106–113. DOI: 10.15406/iratj.2020.06.00209

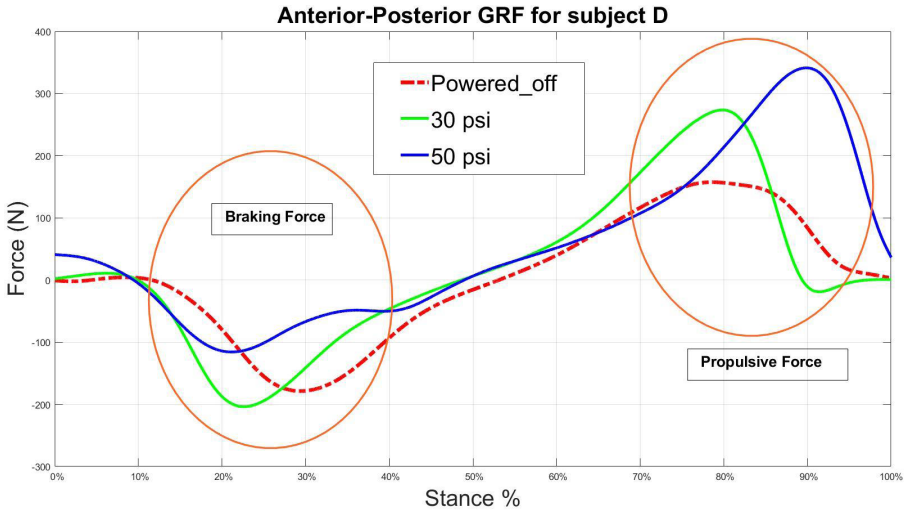

Figure 10 Anterior-Posterior GRF of left leg of Subject D.

Analysis of the GRF data

The results from this preliminary testing of the device show that there is a trend of higher GRF during propulsion with an increase in supply pressure added to the cylinder. For the purpose of this experiment we only analyze the left leg GRF, however during the experiment the subjects were wearing the device on both legs to induce symmetry. This trend of increasing GRF with increase in force is attributed to the force applied to the ball of the foot by the device during push off. The additional push off force increased the anterior-posterior propulsion of the stepping leg. The results from subject A in 7 show that the highest increment of GRF from powered off condition was when a pressure of 30 psi was applied. Subject A revealed during the post session that it felt the most comfortable with 30psi pressure. Subject B, C and D all expressed that they could feel higher push off force with the increase in pressure. Subject A had a variation between 34.87% to 25.43% increase in GRF for the three different applied pressures. Subject B showed a variation between 6.5% to 47% increase in GRF for the different pressures. Subject C showed a variation between 82.44% to 89.61% increase in GRF with the different pressures. Subject D showed a variation of 42.4% to 116.8% increase in GRF with different applied pressures. Different control parameters as mentioned in 1 were used for different subjects and that could have been attributed to the high variation of peaks of the propulsion force. Further testing of the AAFO on a greater number of subjects might show an apparent trend in the relationship between the increase of pressure, control parameters and the GRF.

Conclusion

In this work, we designed an AAFO capable of increasing ground reaction forces of the user all the while being cost effective and comfortable to wear. Individuals who have suffered from stroke have a higher risk of falling and there is evidence that with an active ankle foot orthotic device that is able to provide a strong plantarflexion to the ankle, the individuals would be able to mitigate the factors that cause them to fall. The design of our device utilizes easy to use components and a custom algorithm to provide a stronger push off during normal gait, such that the individuals wearing the device would be able to generate a stronger ground reaction force. Evidence from other studies suggests that a stronger ground reaction force would help in better forward propulsion and would help individuals take faster compensatory steps in the event of a fall. Preliminary tests on the 4 different subjects show a general trend of increase in the anterior-posterior ground reaction forces. There is a need for a comprehensive testing of the device to fine tune the control parameters and make it an effective device that can assist people during an event of a fall.

Funding

The funding for this work was provided by the Brain Center http://brain.egr.uh.edu/.

Acknowledgments

None.

Conflicts of interest

The authors declare that there was no conflict of interest.

References

1. Weerdesteyn V, Niet M, Duijnhoven H, et al. Falls in individuals with stroke. *Journal of Rehabilitation Research And Development*. 2008;45(8):1195–1213.
2. Centres for Disease Control and Prevention. Stroke facts. 2020.
3. Geurts AC, Haart M, van Nes IJ, et al. A review of standing balance recovery from stroke. *Gait & Posture*. 2005;22(3):267–281.
4. Batchelor FA, Mackintosh SF, Said CM, et al. Falls after stroke. *International Journal of Stroke*. 2012;7(6):482–490.
5. Nevisipour M. Evaluating the Effects of Ankle-Foot-Orthoses, Functional Electrical Stimulators, and Trip-specific Training on Fall Outcomes in Individuals with Stroke. 2019.
6. Yamamoto SM, Ebina S, Miyazaki H, et al. Development of anew ankle-foot orthosis with dorsiflexion assist, part 1: Desirable characteristics ofankle-foot orthoses for hemiplegic patients. *Journal of Prosthetics and Orthotics*. 1997;9(4):174–179.
7. Chin R, Hsiao-Wecksler E, Loth E, et al. A pneumatic power harvesting ankle-foot orthosis to prevent foot-drop. *Journal of neuroengineering and rehabilitation*. 2009;6:19.
8. Palmer ML. Sagittal plane characterization of normal human ankle function acrossa range of walking gait speeds. *MIT*. 2002.

9. Hwang S, Kim J, Yi J, et al. Development of an active ankle foot orthosis for the prevention of foot drop and toe drag. *International Conference on Biomedical and Pharmaceutical Engineering*. 2006;418–423.

10. Boehler AK. Hollander KW, Sugar T, et al. Design, implementation and test results of a robust control method for a powered ankle foot orthosis (afo). *IEEE International Conference on Robotics and Automation*. 2008:2025–2030.

11. Polinkovsky A, Bachmann RJ, Kern N, et al. An ankle foot orthosis with insertion point eccentricity control. *IEEE/RSJ International Conference on Intelligent Robots and Systems*. 2012;10:1603–1608.

12. Ferris DP, Czerniecki JM, Hannaford B. An ankle-foot orthosis poweredby artificial pneumatic muscles. *Journal of applied biomechanics*. 2005;21(2):189–197.

13. Quintero D, Lambert DJ, Villarreal DJ, et al. Realtime continuous gait phase and speed estimation from a single sensor. *IEEE Conference on Control Technology and Applications (CCTA)*. 2017:847–852.

14. Qi H, Bone GM, Zhang Y. Position control of pneumatic actuators using three-mode discrete-valued model predictive control. *Actuators*. 2019;8(3):56.

15. Taborri J, Palermo E, Rossi S, et al. Gait partitioning methods: A systematic review. *Sensors*. 2016;16(1):66.

16. Watanabe T, Saito H, Koike E, et al. A preliminary test of measurement of joint angles and stride length with wireless inertial sensors for wearable gait evaluation system. *Computational Intelligence and Neuroscience*. 2011:411–422.

Citation: Olson J, Ray S, Sugar T, et al. Design of active ankle foot orthotics for gait assistance and fall prevention. *Int Rob Auto J.* 2020;6(3):106–113.
DOI: 10.15406/iratj.2020.06.00209